18. CRYSTAL MORPHOLOGIES IN BASALTS FROM DSDP SITE 395 23° N, 46° W, MID-ATLANTIC RIDGE

James H. Natland, Deep Sea Drilling Project, Scripps Institution of Oceanography, La Jolla, California

INTRODUCTION

At DSDP Site 395, a sequence of basaltic pillow lavas, thin basaltic flows, and intrusive basalts was drilled in two holes, along with minor gabbroic and ultramafic rocks (Chapter 7, this volume). Both aphyric and strongly phyric basalts were recovered. The latter include both plagioclase-olivine phyric and plagioclase-olivine-clinopyroxene phyric basalts. The aphyric and phyric basalts were designated types A and P, respectively, on the basis of chemical and magnetic stratigraphy (Chapter 7, this volume). Three aphyric (A_2 through A_4) and five phyric (P_1 through P_5) basalt types were defined. Their general stratigraphy is shown in Figure 1, together with the correlation between Holes 395 and 395A. Originally, an additional aphyric basalt type, A_1, was defined on the basis of one chemical analysis (shipboard data, Bougault et al., this volume); but shore-based analyses later demonstrated that similar rocks occur sporadically throughout Unit A_2, so the two types were combined (Chapter 7, this volume). In addition, intrusive rocks deeper in Hole 395A are designated type P_4', indicating close chemical similarity to Unit P_4 higher in the hole. The two units also have the same magnetic inclination (Figure 1).

Each chemical unit can consist of glassy or near-glassy pillow fragments, coarser grained pillow interiors and, in some cases, thicker flows (e.g., Unit P_3, Figure 1). Some units contain fracture breccias or glass breccias (P_5, A_3, and A_4). All are altered and fractured to greater or lesser degrees. The one common characteristic of each unit, however, is not its lithologic variability, but its internal chemical coherence (Chapter 7, this volume; Bougault et al., this volume).

The texture of basalts in any given unit can vary considerably. The range of crystal morphologies depends largely on what portion of a pillow rim or interior is examined, but it also depends on chemistry. Near the glassy rims of pillows, spectacular spherulitic to skeletal crystals can be seen in thin sections, a consequence of the high degrees of undercooling when the molten lavas were extruded as pillows or thin flows into the frigid water of the deep sea floor. Within the pillow or flow interiors, the rocks are more holocrystalline, and most crystals have euhedral, tabular, or granular forms.

This paper is essentially a pictorial display, with commentary, of silicate crystal morphologies in Site 395 basalts. By means of photomicrographs, I will illustrate the cooling history of the basalts, the dependence of crystal morphologies on undercooling and on surprisingly small differences in chemistry, and the significance of phenocrysts in the phyric basalts on their petrogenesis. For discussion of opaque minerals, see Johnson (this volume), and for spinels, Graham et al. (this volume).

Much of the interpretation in this paper depends critically on the chemical, mineralogical, and experimental work of other contributors to this volume. I hope that these photomicrographs will extend and clarify many of their conclusions. The terminology for crystal morphologies adopted herein is primarily that of Lofgren (1971, 1974) for spherulitic forms in general and Donaldson (1976) for olivines. Some of the terms of Bryan (1972) are also used.

The emphasis here is not so much on particular minerals or particular crystal morphologies as on mineral interrelationships. Samples from deep-penetration DSDP sites are particularly suited for this type of study because stratigraphic control is superb, because all ranges of crystal morphologies of particular chemical types occur, and because a good variety of chemical types closely related in time and space can be examined.

CRYSTAL MORHPOLOGIES IN APHYRIC BASALTS

The type A_2 aphyric basalts, present in both Hole 395 and Hole 395A, are pillows, each commonly with a variolitic zone, a vesicular zone, and a chilled, but rarely glassy, rind. Textures range from extremely fine grained to coarsely microlitic, but very little true glass was found.

The reason for this appears related to the unusually large (up to 1 cm) variolites abundant in these basalts. "Variolites" here is a term used in much its original sense: "spherical bodies appearing on the weathered surfaces or marginal portions of certain diabases" (quoted from Lofgren, 1974, his table 2, after Johannsen, 1939). A typical piece of basalt from aphyric Unit A_2 is shown in Figure 2, along with representative photomicrographs showing textures and crystal morphologies with increasing distance away from inferred quench margins. The variolites themselves are mats or sworls of extremely fine plagioclase needles, dotted with opaques, and criss-crossed with altered linked-chain (terminology of Donaldson, 1976) or "lantern and chain" olivine (terminology of Bryan, 1972). These are shown in Figure 2B.

The material surrounding the variolites is buff in color, apparently the result of oxidation of glass or titanomagnetite to clays and iron oxyhydroxides. Altered linked-chain olivines are still present, but the

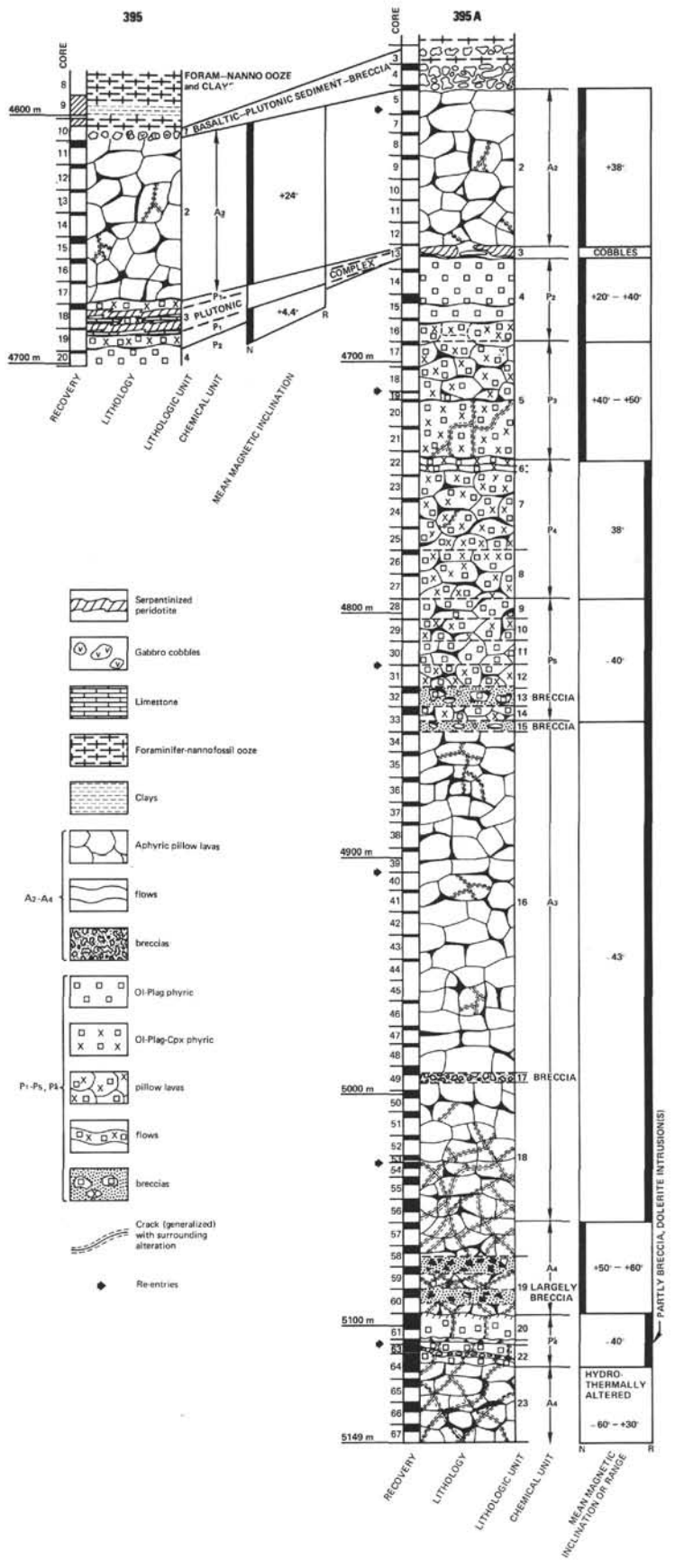

Figure 1. *Basement stratigraphy, Site 395.*

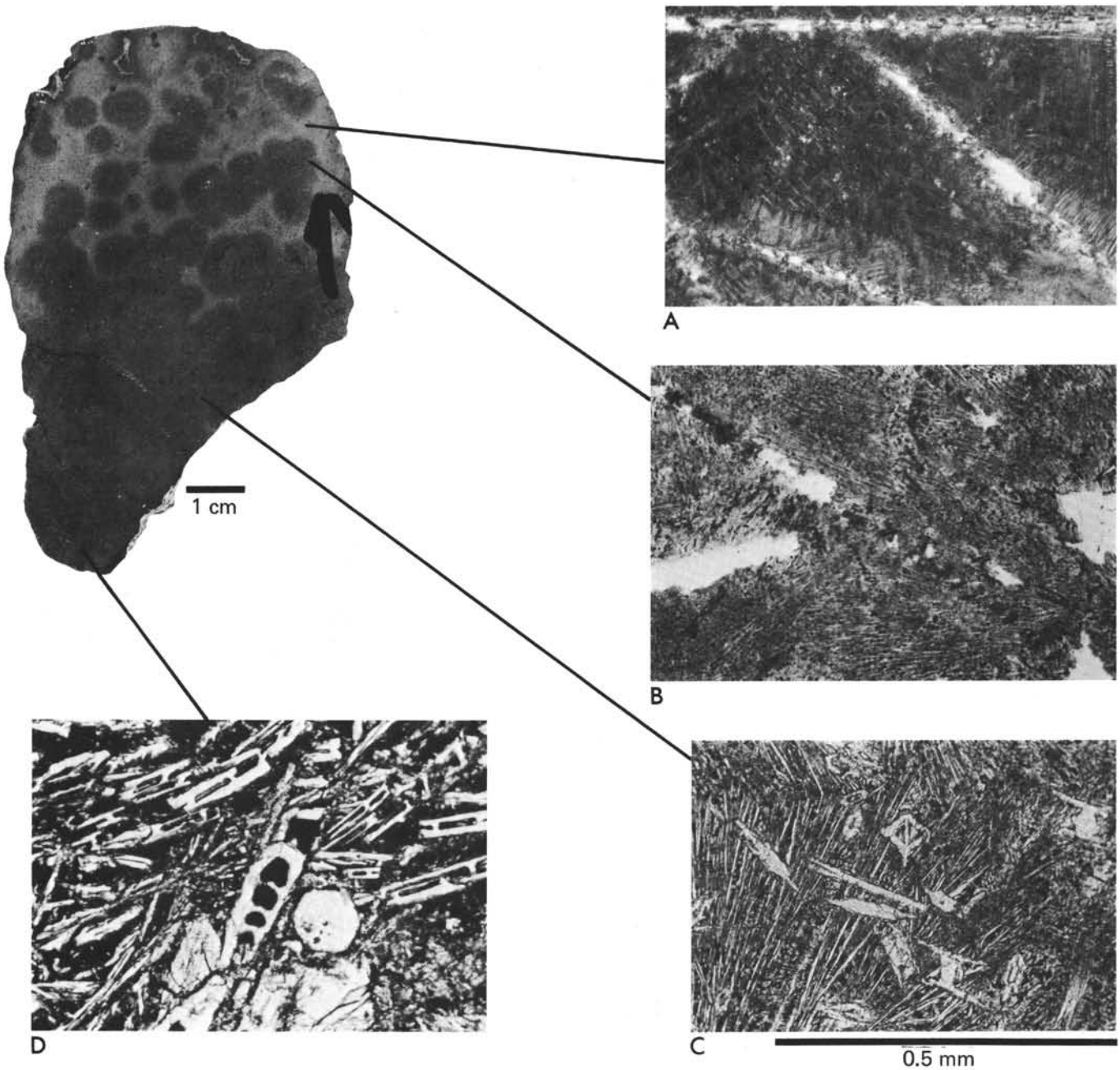

Figure 2. *Crystal morphologies in basalts of Unit A_2. Unit A_2, aphyric basalt, is a series of pillow lavas with abundant evidence for extensive undercooling under water. The large photograph shows a single piece with large "variolites" (dark gray patches) surrounded by much finer grained basalt. The increase in grain size toward the cooling-unit interior is shown by the photomicrographs, all to the same scale. Photo A shows extremely elongate linked-chain olivines in a matrix of acicular plagioclase microlites. Photo B, the interior of one of the variolites, is somewhat coarser grained, and has abundant titanomagnetite in addition to acicular plagioclase. Photo C, taken away from the variolitic zone, shows ornamented "hopper crystal" olivines, less elongate than in A or B, in a matrix of acicular plagioclase and titanomagnetite. Photo D represents about the coarsest grain size recovered in this unit. The central crystals are granular or skeletal olivines. They are surrounded by skeletal plagioclase enclosing clinopyroxene, titanomagnetite, or glass. Sample numbers: Photos A and B: 395A-9-1, 128-138 cm (#3). Photo C: 395A-7-1, 75-77 cm (#3). Photo D: 395-15-2, 130-136 cm (#3B). Basalt piece is Sample 395-16-2, 37-45 cm (#7). Top is shown by arrow on piece.*

fine plagioclase needles in the matrix are so fine as to be barely discernible (Figure 2A). The variolites therefore appear to be centers of nucleation which formed at slightly lesser undercoolings than the extreme edges of the cooling units.

Coarser grained portions of cooling units contain very elongate, possibly dendritic, plagioclase microlites. Olivine crystals are better formed, fresh, and not so elongate (Figure 2C). They conform to the "hopper crystal" morphology of Donaldson (1976).

Titanomagnetite is skeletal and abundant. Clinopyroxene, if present, is in the spaces between the plagioclase crystals; its morphology cannot be discerned.

The coarser grained basalts of aphyric Unit A_2 contain subhedral to skeletal olivine up to 0.5 mm long, discernible in hand specimens (Figure 2D). These are in a matrix of stubby to elongate skeletal plagioclase crystals, each with one or more hollow interior spaces filled with probably dendritic augitic clinopyroxene and skeletal titanomagnetite. This material also surrounds the exterior of the plagioclase crystals. The plagioclase has tended to nucleate on the larger olivine crystals, from which it grows in radial sworls. For most sworls, however, no nucleating agent can be seen.

The contrasts between aphyric Unit A_2 and aphyric Units A_3 and A_4 is subtle chemically (Chapter 7, this volume; Bougault et al., this volume), but distinct petrographically. Figure 3 shows a series of photomicrographs, paralleling the sequence of Figure 2, from glassy rims to coarser interiors. Units A_3 and A_4 are quite similar petrographically, and are here described together. Unlike Unit A_2, in which virtually no glass was found, Units A_3 and A_4 contain abundant glass, including a thick glass breccia zone (lithologic Unit 19 of Hole 395A, table 3 in Chapter 7, this volume). The glass is clear and pale brown, with tiny crystallites of olivine that have tiny swallow-tail arms radiating from the corners (Figure 3A). The crystallites are surrounded by fine feathery spherulitic halos which are more readily seen in cross-polarized light (Figure 3B). About 0.5 to 1 cm farther toward cooling unit interiors, these are joined by dark brown to black spherulites about 0.05 mm in diameter. These often are arranged in curved rows, paralleling the glassy margin (Figure 4). About 0.5 cm farther into cooling units, these spherulites become predominant, and contain in their centers tiny plagioclase microlites which often have swallow-tail arms merging with the brown spherulitic overgrowths. Fibers within the spherulites can be dendritic (Figure 3C). Between about 2 and 5 cm from glassy edges, plagioclase becomes distinctly skeletal and elongate, having grown radially from nucleation centers such as olivine (Figure 3D). But it does not reach the extreme c-axis elongation of plagioclase in aphyric Unit A_2. Clinopyroxene forms spherulitic patches between the radiating plagioclase grains, and also occurs within the elongate axial hollows of the skeletal plagioclase. Titanomagnetite, which is not evident in the glassy and spherulitic zones of typical A_3 and A_4 basalts, first occurs here.

In the coarser grained rocks (which are finer grained than any basalts in Unit A_2), stubby euhedral to elongate skeletal plagioclases are intergrown with granular olivine, and surround later-grown pale brown augitic clinopyroxene, skeletal titanomagnetite, and patches of brown glass (Figure 3E).

The striking contrast in crystal morphologies between coarser grained microlitic basalts of aphyric Units A_2 and A_3 can be seen in Figure 5, which compares two samples with well-developed skeletal plagioclase. The A_2 basalt is distinctly coarser grained than the A_3 basalt (we recovered no A_3 basalts much coarser grained than that shown in Figure 5), yet the skeletal plagioclase habit and c-axis elongation is much more pronounced.

Table 1 summarizes the sequence of crystallization of minerals and their morphologies with increasing distance into cooling units. The morphologic changes in general conform to those predicted experimentally for both olivine (Donaldson, 1976) and plagioclase (Lofgren, 1974) at decreasing undercoolings. The differences between the two types of aphyric basalt appear to arise primarily because the aphyric basalt Units A_3 and A_4 are more fractionated than Unit A_2 (Bougault et al., this volume; Rhodes et al., this volume). A_2 basalts have both more Fe (as FeO*) and more MgO than A_3 and A_4 basalts, so are more prone to crystallize olivine. Olivine is not only more abundant in the A_2 basalts than in the others, but its apparent abundance is enhanced at higher undercoolings (note abundant "hopper" olivines in Figure 2C). The higher total iron may also explain why the titanomagnetite/clinopyroxene crystallization sequence is reversed at higher undercoolings in the A_2 basalts, and why titanomagnetite occurs so much closer to cooling unit boundaries than in the A_3 and A_4 basalts. A similar reversal of crystallization sequence between plagioclase and ilmenite was obtained at high undercoolings in experiments on a lunar picritic basalt by Walker et al. (1976). There is no completely obvious reason why crystal morphologies at about the same distance from cooling unit boundaries seem to differ between the A_2 and A_3-A_4 basalts (linked-chain olivine nearest A_2 cooling unit boundaries versus swallow-tail olivine in a similar zone in the A_3 and A_4 basalts, for one example, and extreme c-axis elongation in the A_2 basalts but not in the A_3 and A_4 basalts, for another). The causes are probably compositional, but could also be related to melt viscosity (a function in part of volatile contents), or P_{O_2}. Some combination of factors limited the diffusion rate at all levels of undercooling in the A_2 basalts more effectively than in A_3 and A_4 basalts, inhibiting formation of polyhedral crystals in the coarser grained basalts, and of all but needle-like crystals in the finer grained basalts. No well-defined centers of nucleation could develop in the finer grained A_2 basalts, so the large variolites grew near the chilled margins. All these morphologies appear to result from high undercooling, since a range of crystal morphologies similar to that in A_3 basalts was produced experimentally at cooling rates between 2°/hr and 30°/hr by Dungan et al. (this volume).

CRYSTAL MORPHOLOGIES IN PHYRIC BASALTS

Phyric basalts in Hole 395 can be divided into two types (Figure 1): an upper plagioclase-olivine-clinopyroxene phyric group (Core 18, chemical type P_1) and a lower plagioclase-olivine phyric group (Cores 19 and 20, chemical type P_2). P_1 is not present in Hole 395A, but P_2 extends from Core 13 to Core 16. Chemical type P_3 (Cores 17 through 22) is once again plagioclase-clinopyroxene-olivine phyric, as is P_4 (Cores 22 through 27). Phyric Unit P_5 (Cores 28 through 33) contains mainly plagioclase and olivine phenocrysts, but

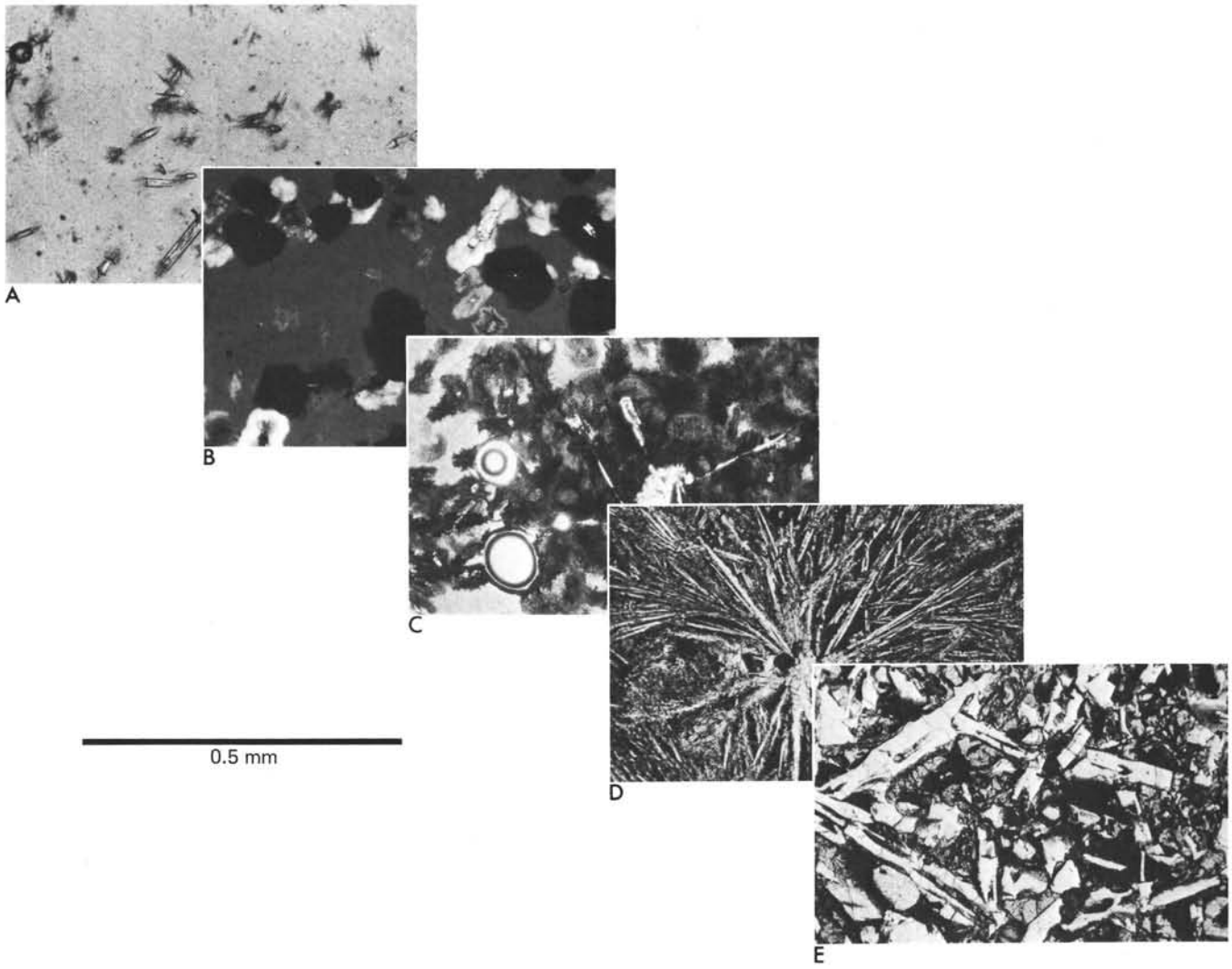

Figure 3. *Crystal morphologies in basalts of Units A_3 and A_4 (A_3 illustrated). Photos A through E represent typical textures from glassy margins to cooling-unit interiors. Glasses typically contain tiny crystallites of olivine* (A) *with bright "halos" in cross-polarized light* (B). *Incipient plagioclase crystallites form the interiors of the darker spherulites in* (B), *and become crowded and less spherical toward the cooling-unit interior* (C). *The individual fibers of spherulites in* (C) *can be dendrites. Still farther into cooling units, radiating acicular plagioclase bundles emenate from olivine nuclei and enclose incipient clinopyroxene* (D). *The coarsest grained rocks show granular olivine and skeletal plagioclase, and partially skeletal clinopyroxene and titanomagnetite. Note contrast in behavior of crystals closest to quench margins between Units A_2 (Figure 2) and A_3. Sample numbers: Photos A and B: 395A-56-3, 94-96 cm (#11). Photo C: 395A-55-2, 137-138 cm (#8). Photo D: 395A-17-1, 102-107 cm (#12). Photo E: 395A-55-2, 72-75 cm (#3D).*

Figure 4. *Sample 395A-56-3, 94-96 cm. Aligned plagioclase spherulites in glassy rim of Unit A_3 pillow. Transmitted light. Width of figure at top is 1.4 cm. Note palagonite at edge of glass and small plagioclase crystal to left of center.*

Cores 29, 31, and 33 have minor clinopyroxene phenocrysts.

A general description of these rocks was given in Chapter 7 (this volume) as follows: "In general, these phyric units are characterized by an abundance of euhedral plagioclase phenocrysts, up to 25 per cent in parts (visual estimate), with about 7 per cent olivine and minor clinopyroxene. A number of thin sections, made from hand specimens in which pale emerald green clinopyroxenes were seen, either with the unaided eye or using a binocular microscope (×6), have no clinopyroxene phenocrysts when examined microscopically, because the distribution of clinopyroxene as a phenocryst phase is patchy. In Cores 13 through 15, none was visible either in hand specimen or in thin section. These fine-grained phyric basalts contain as phenocrysts about 20 per cent plagioclase, An_{75} (0.3 to 0.5 cm across), and 7 per cent olivine ($\sim Fo_{85}$, $2V \sim 90°$) 0.3 cm across, set in a holocrystalline groundmass of clinopyroxene ($2V \sim 60°$), olivine, lath plagioclase, and titanomagnetite. The feldspar phenocrysts show both normal and oscillatory zoning, and often contain inclusions of brown glass as blebs in their cores. In Cores 16 through 22, clinopyroxene is present as a phenocryst phase, and rare, rounded, dark brown spinel occurs" (it also occurs in Units P_4 and P_5).

There are two generations of plagioclase crystals in all these phyric basalts. Large phenocrysts (0.3 to 0.5 cm long) have cores with compositions of around An_{86-83} (Dungan et al., this volume) and rims of An_{73-62}. They often show simple albite twinning, and the cores almost always have abundant glass inclusions (Figure 6A). In the coarser grained rocks, these inclusions are finely crystalline (Figure 6B), but nearer cooling unit boundaries they are still glass. The more sodic rims of these crystals have only minor glass inclusions (Figure 6C and D). In the coarser grained rocks (sub-ophitic to gabbroic textures), the rims can have extremely irregular terminations (Figure 6A), and the sides of some crystals are plated with smaller plagioclase crystals which apparently grew by heterogeneous nucleation (Figure 7). In spherulitic and glassy basalts, the sodic rims have no inclusions, but under conditions of high undercooling (upon extrusion of pillows from larger flows?), they are dendritic (Figures 6C and D). In these basalts the more sodic rims also tend to have more "squared-off" morphologies than the crystals they surround (Figure 6E). The surrounded crystals can have rounded outlines, suggesting that they were first partially resorbed (Figure 6E).

The more sodic rims are compositionally identical to the range of compositions of the second generation of plagioclase phenocrysts in the phyric basalts, and are therefore part of that second generation. Crystal morphologies of single second-generation plagioclase phenocrysts are simple, and tend to be square or rectilinear in glassy rocks (Figure 8A), with at most a single twinning plane within them. Some are skeletal (Figure 8B). In some basalts there are glomerophyric clumps of plagioclase with more complex twinning (Figure 8C), but these too belong to the more sodic generation of phenocrysts. The crystal clumps can have feldspars

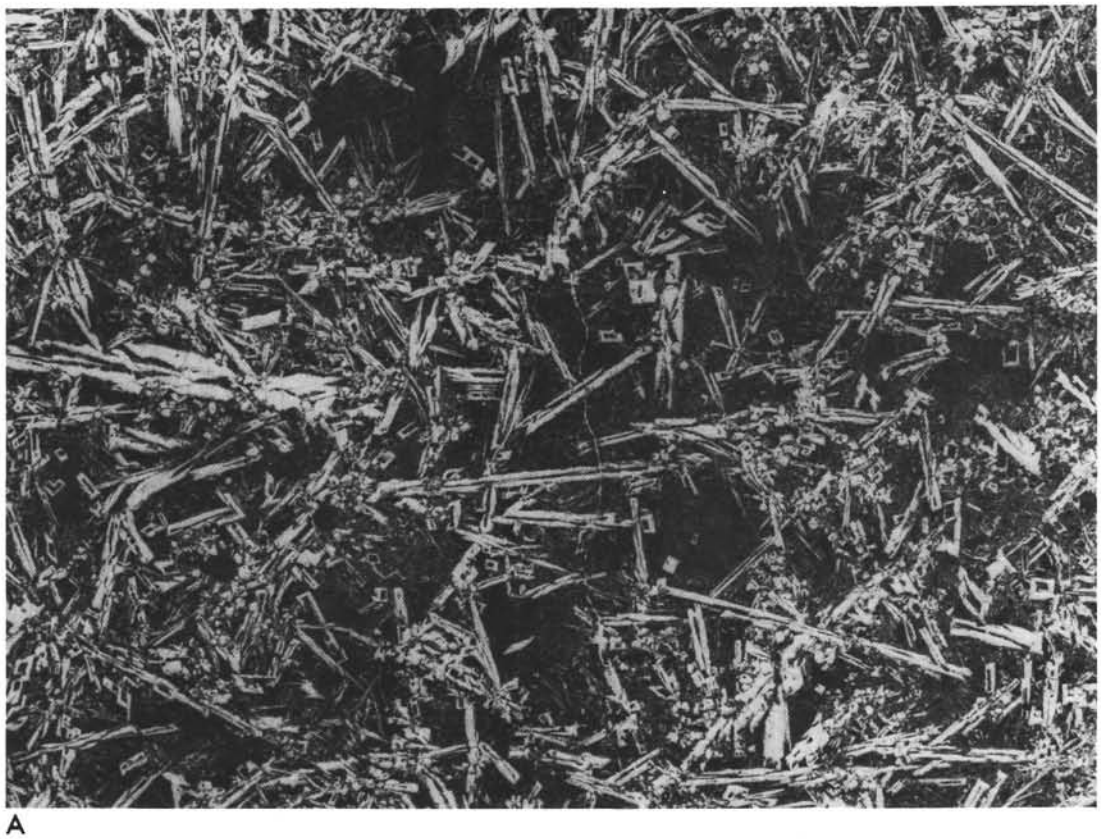

A

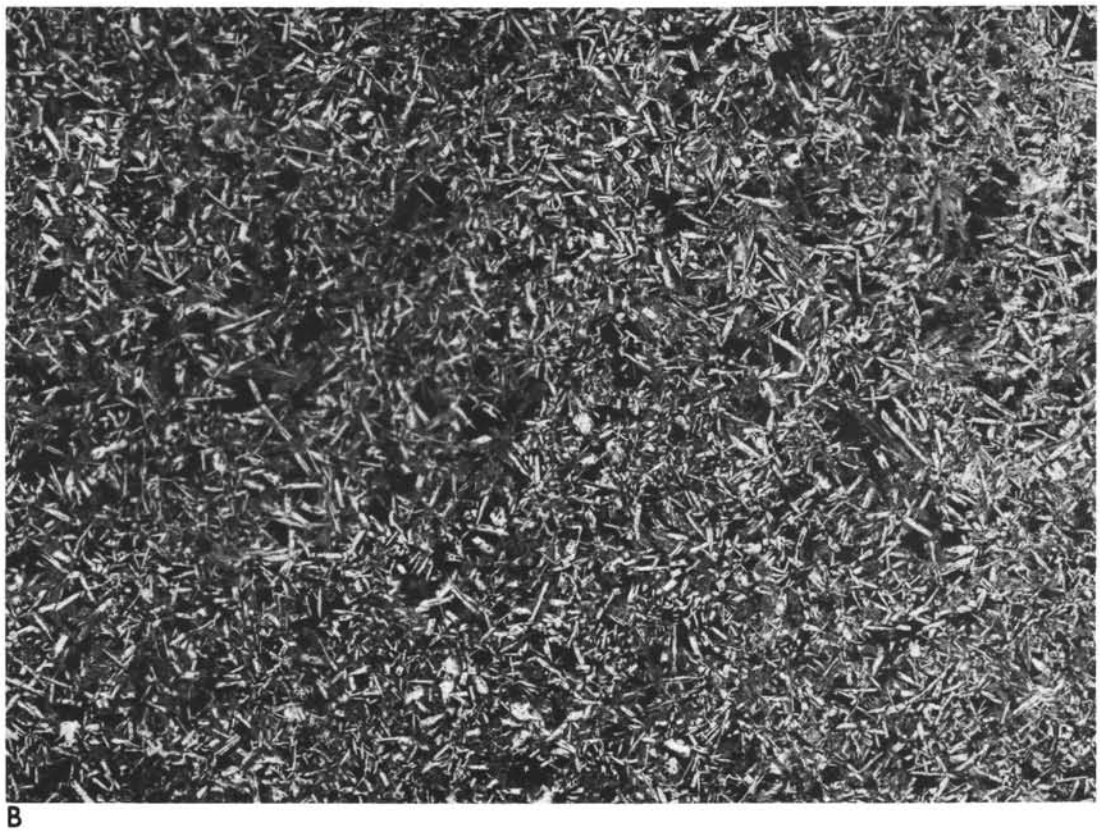

B

Figure 5. (A) *Sample 395A-5-1, 100-102 cm (#16D), Unit A_2. Transmitted light. Long dimension = 3 cm.* (B) *Sample 395A-55-2, 72-75 cm (#4), Unit A_3. Transmitted light. Long dimension = 2.9 cm.*

TABLE 1
Sequence of Crystallization and Crystal Morphologies in Site 395 Aphyric Basalts as They Vary With Distance From Cooling Unit Boundaries

	A_2	A_3-A_4
0-1 cm	1) Olivine (linked-chain) 2) Plagioclase needles and sworls Rare glass (glassiest zones have spherulitic plagioclase and iron oxyhydroxides)	1) Olivine (swallow-tail and feathery) Glass
~1-10 cm	1) Olivine (linked-chain to hopper crystals) 2) Plagioclase needles (in variolites) 3) Titanomagnetite	1) Olivine (swallow-tail to granular) 2) Plagioclase (spherulites to radial clumps)
> 10 cm	1) Olivine (granular) 2) Plagioclase (skeletal and large) 3) Clinopyroxene (tiny and dendritic(?)) 4) Titanomagnetite (skeletal)	1) Olivine (granular) 2) Plagioclase (skeletal to euhadral) 3) Clinopyroxene (dendritic) 4) Titanomagnetite (skeletal)

Decreasing undercooling ↓

Note: Numbers by each mineral indicate order of crystallization.

stacked upon each other sideways (Figure 8D), or they can be randomly oriented (Figure 8E). The first type may have grown by heterogeneous nucleation, perhaps promoted by flow of the basalt (note parallel orientation of many plagioclase phenocrysts in Figure 9). The more randomly oriented kind may have grown within a magma chamber where magma movements were either minor or turbulent, and in any case not laminar. Magma movements may also be indicated by second-generation plagioclase with fine oscillatory zoning (Figure 8F).

Of the two types of plagioclase phenocrysts, the more sodic variety is perhaps an order of magnitude more abundant numerically. But because they are so much smaller (0.1 to 1 mm) than the calcic types, the volume proportions of the two types are probably about the same (Figure 9).

Olivine and clinopyroxene phenocrysts are much less abundant than plagioclase phenocrysts, and it is not always clear with which generation of plagioclase they might have crystallized. Most olivine apparently belongs with the older generation of plagioclases. Dungan et al. (this volume) found the olivine in phyric basalts to be distinctly more forsteritic than olivine grown under equilibrium conditions at low pressure from whole-rock starting compositions. (They also noted that plagioclase grown in the same experiments was more sodic than the cores of the large phenocrysts.) Glass inclusion compositions from both olivine and plagioclase phenocrysts are also less evolved than the glass from quickly chilled rims of the phyric basalts (Fujii et al., this volume; Rhodes et al., this volume). This complex of data suggests to Rhodes et al. (this volume) and Dungan et al. (this volume) that the first (more calcic) generation of plagioclase phenocrysts, as well as the olivine, grew in a more primitive melt than that represented by the bulk composition of the phyric basalt types or their phenocryst-free glasses. They propose that this primitive magma, charged with phenocrysts, invaded one or more magma chambers containing substantially more fractionated basalts, and that the phyric basalt types therefore are a hybrid of at least two distinct magma types.

Because spinel and clinopyroxene compositions in the experiments conformed with those in the basalts, Dungan et al. (this volume) thought them to be "probably not exotic to these rocks." Spinels and clinopyroxene therefore appear to belong for the most part to the second generation of phenocryst minerals.

In one respect, the experiments oversimplify interpretation of the growth of phenocrysts in the phyric basalts. The experiments were done on whole-rock compositions, not on either of the inferred end-members, "primitive" or "evolved," of which the whole rocks appear to be hybrids.

The experiments were also done on a sample from Unit P_4, which has a more fractionated composition than Units P_1 and P_3, and differs from them in that clinopyroxene phenocrysts are scarce or absent (Chapter 7, this volume). The experiments therefore apply mainly to the more evolved plagioclase and olivine phyric units P_2, P_4, and P_5. There appear to be, in fact, two different types of olivine phenocrysts and several different types of clinopyroxene phenocrysts in the phyric basalts (Figure 10).

In some basalts, olivine can occur as large whole megacrysts with fractured and cracked edges (Figure 10A). These appear to be "first-generation" olivine. At the time of extrusion, they were not growing in their surroundings, and were too magnesian to have been undergoing resorption (assuming they were "mixed" into a more fractionated liquid than that in which they originally grew). The edges, however, appear to be mechanically disintegrating. Also, in sinking or otherwise moving through their originally molten surroundings, many have "collected" clusters of other crystals around them, as in Figure 10A. In other basalts, olivine phenocrysts can be euhedral, and enclose plagioclase crystals.

Other olivines are distinctly skeletal, conforming to the "granular" or "hopper-crystal" terminology of Donaldson (1976). These crystals are considerably larger than their morphological equivalents in the aphyric basalts. Some, indeed, are several millimeters in diameter, and contain "cavernous" round or oval glass or groundmass inclusions (Figure 10B). Others have

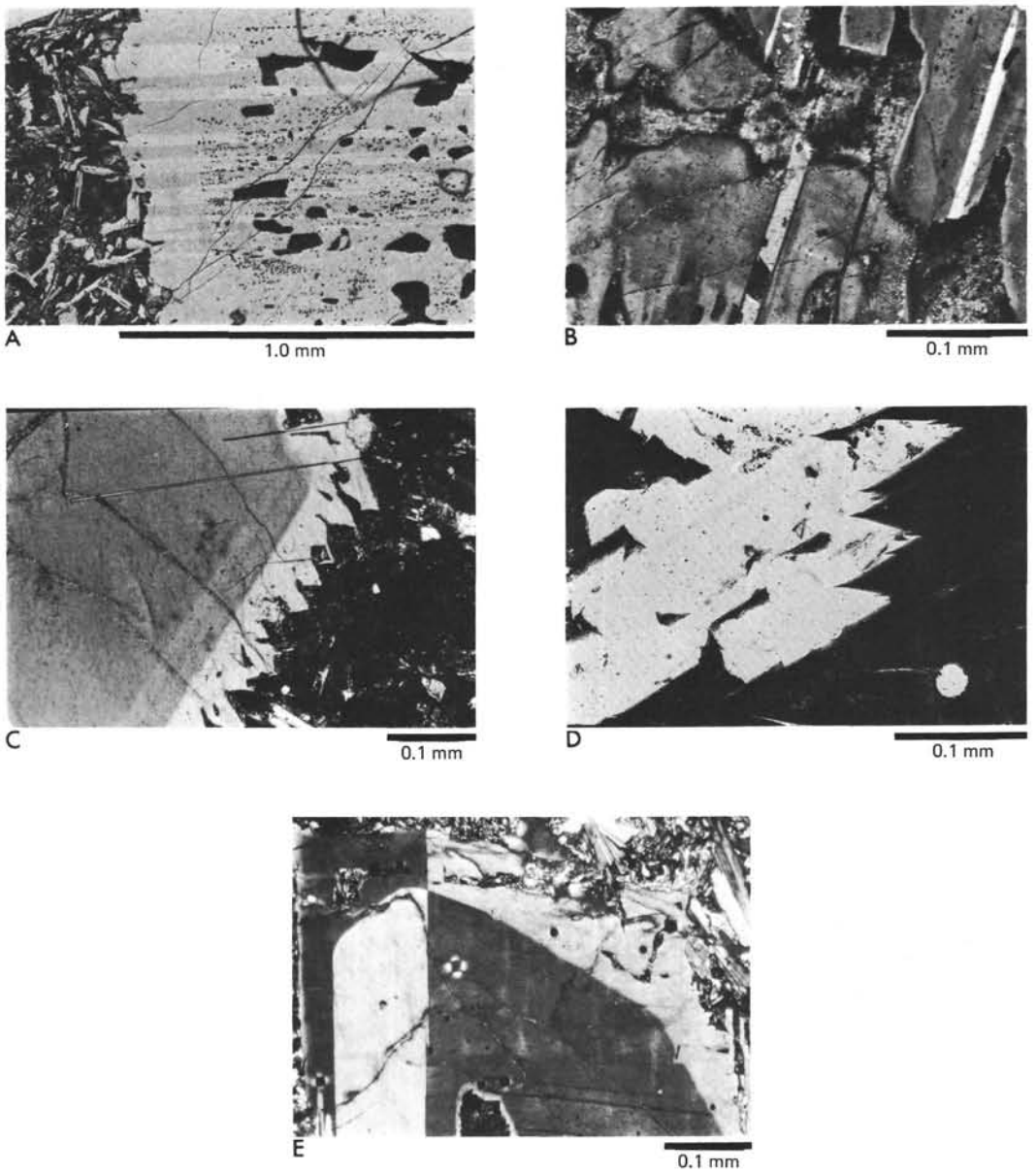

Figure 6. *(A) Sample 395-18-1, 37 cm (#1), Unit P_1. Crystal showing internal skeletal structure (glass inclusions) indicative of initial period of high undercooling, a zone of stable growth (no glass inclusions), and a zoned dendritic rim, grown at high undercooling (pillow extrusion) Plane light slightly cross-polarized to show twinning. (B) Same sample as in A, showing detail of spherulitic crystal growth within inclusions in plagioclase phenocryst. Crossed nicols. (C) Same sample as in A, showing "staircase" dendritic overgrowth in sodic rim of sharply zoned phenocryst. Note how merging of dendritic overgrowths results in skeletal inclusions of groundmass. Also note thin twin lamellae paralleling shorter faces of overgrowth. Crossed nicols. (D) Sample 395A-17-1, 131-135 cm (#15D), Unit P_2. "Staircase" dendritic crystal margin and skeletal inclusions in sodic plagioclase microphenocryst. Flared tips of overgrowths indicate even higher undercoolings as the rock was rapidly chilled upon extrusion. Plane light. (E) Sample 395-19-1, 36-38 cm (#4), Unit P_2. Sharply zoned plagioclase phenocryst with spherulitic inclusion at bottom. The rounded edges of the inner zone suggest that resorption was followed by overgrowth of a more sodic rim, first at relatively small undercoolings, then at larger undercoolings, to produce the "squared-off" crystal boundary, which trapped inclusions of groundmass material.*

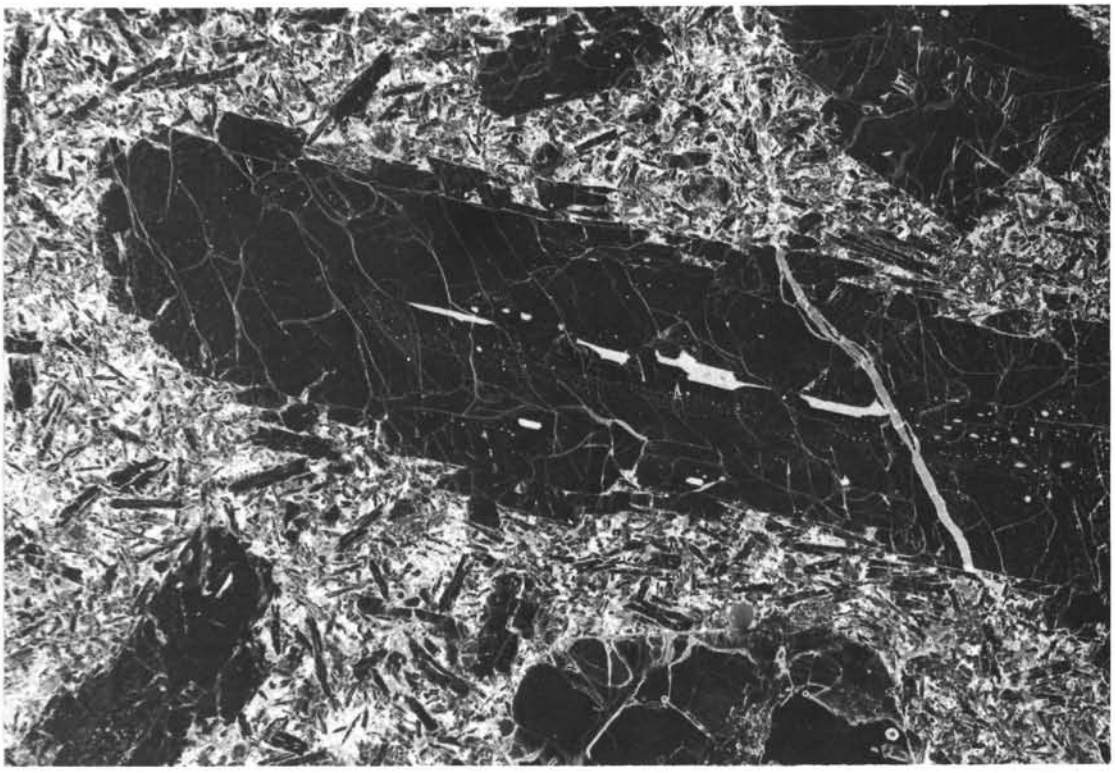

Figure 7. *Sample 395A-15-1, 13-17 cm (#1D), Unit P_2. Large plagioclase crystal in center is 3.2 mm at its widest part. The negative image was taken by putting the thin section directly in an enlarger, and exposing print paper directly. Extremely fine details, such as strings of very tiny melt inclusions in the plagioclase, can be resolved in this way. Core of large plagioclase has composition An_{88}; rim is An_{78}. Olivine at bottom is F_{090} (J. Natland, unpublished data). Large dark glass inclusions in center of plagioclase are here prominently white. The crystal is plated with smaller second-generation plagioclase crystals.*

outlines which suggest the more typical dome or prismatic forms of olivine (Figures 10C and 10D). These are invariably associated with second-generation plagioclase, similar in size and even in morphology, tending to be simple euhedral to skeletal crystals (Figure 10D). Rarely, small euhedral olivines can be seen, some with sector zoning (Figure 10E).

The various types of clinopyroxene phenocrysts are exemplified by Figure 11A, which shows a rounded phenocryst with a rim of intergrown plagioclase and clinopyroxene; a large second-generation plagioclase phenocryst is at the upper right. Figure 11B shows details of a similar clinopyroxene-plagioclase rim on a larger phenocryst. The clinopyroxene in the rim has grown dendritically from the core, but the attached plagioclase crystals have a somewhat random orientation. The material outside the crystal is extremely fine grained, and crystallized at fairly high undercoolings. The intergrowth of clinopyroxene and plagioclase at the phenocryst rims suggest that, at the high undercoolings in which the dendritic rim formed, crystallization of the clinopyroxene locally enriched the residual liquid in the components of plagioclase, which therefore grew in whatever remaining space it could find.

A smaller version of a two-stage clinopyroxene is shown on Figure 11C. This clinopyroxene shows sector zoning and has a distinct rim. Rims of clinopyroxene such as this are both normal and reversely zoned with respect to the crystal interiors (Fujii and Fujioka, this volume).

Figure 11D shows one final example of a clinopyroxene phenocryst. This one is axially intergrown with a plagioclase phenocryst. It also shows strong radial compositional zoning about its intersection with the plagioclase grain. This almost certainly reflects compositional gradients induced by the strong partitioning of Ca into the plagioclase.

There appear, then, to be several different stages of crystallization represented by olivine and clinopyroxenes in the phyric basalts. The olivines represent at least two stages. The first consists of the more forsteritic variety, which occurs as granular megacrysts, sometimes with tattered edges, sometimes euhedral. These correspond in many cases to the first generation of plagioclase phenocrysts. The second consists of the skeletal olivine "hopper" crystals, or sector-zoned crystals, which grew simultaneously with the more sodic second-generation plagioclases. Among the clinopyroxenes occur compositionally uniform granular phenocrysts with dendritic edges, normal- and reversely-rimmed, sector-zoned phenocrysts, and unrimmed radially-zoned phenocrysts intergrown with late-stage plagioclase. Clinopyroxene is also a major groundmass phase. In the more fractionated phyric basalts (Units

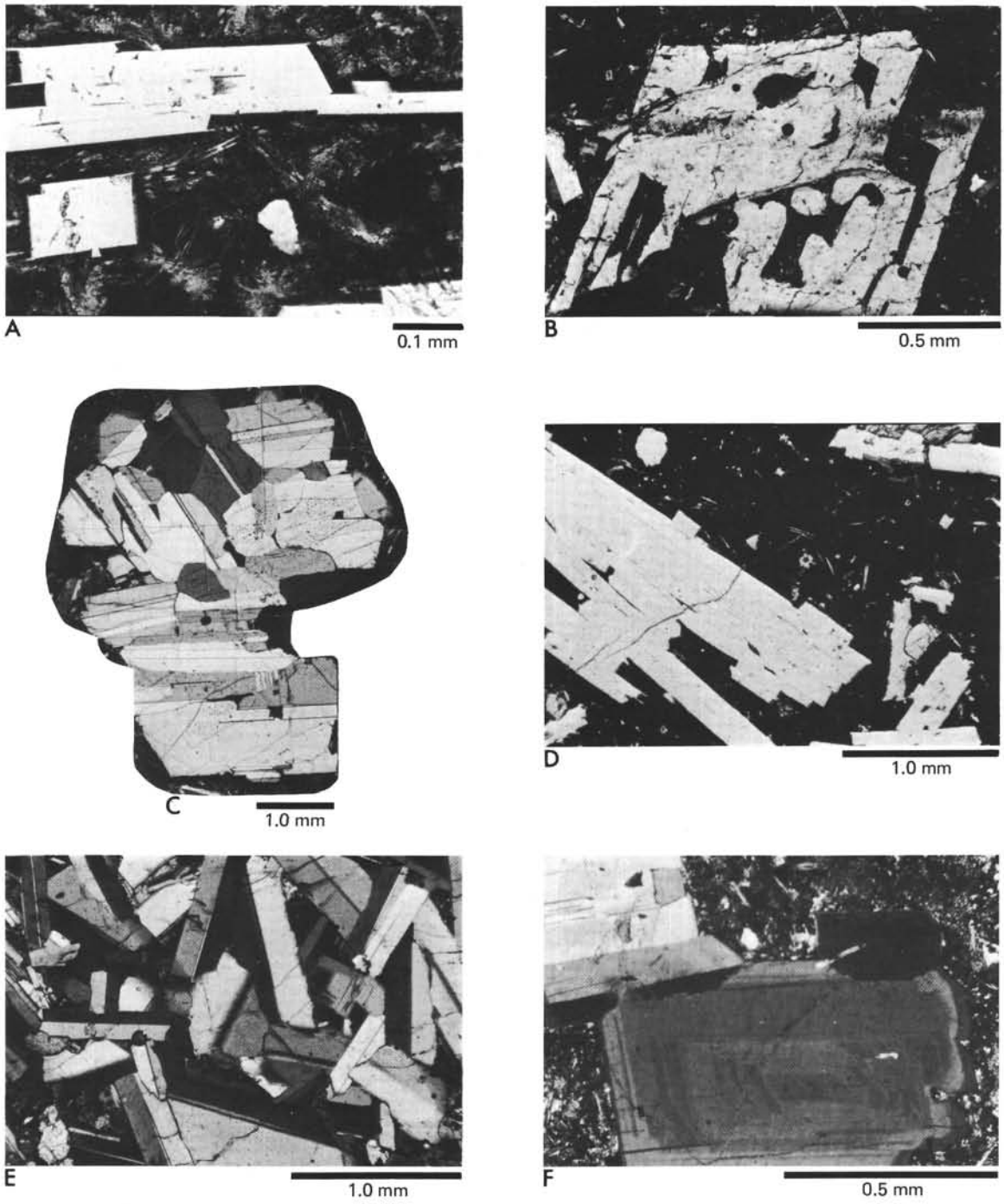

Figure 8. (A) *Sample 395A-17-1, 131-135 cm (#15D), Unit P_5. Plane polarized light. Tabular plagioclase crystals joined lengthwise in spherulitic groundmass. Note thin dendritic projections at corners of the crystals.* (B) *Sample 395A-17-1, 131-135 cm (#15D), Unit P_3. Skeletal second-generation plagioclase crystal in same sample as A. Plane polarized light.* (C) *Sample 395-20-1, 32-36 cm (#5), Unit P_2. Crossed nicols. Composite photomicrograph of a large plagioclase glomerocryst.* (D) *Sample 395-18-2, 38 cm (#7), Unit P_2. Plane polarized light. Synneusis cluster of tabular second-generation plagioclase microphenocrysts.* (E) *Sample 395A-15-1, 93-94 cm (#10), Unit P_2. Crossed nicols. Central portion of a large second-generation plagioclase glomerocryst in which most crystals are at irregular angles to one another.* (F) *Sample 395A-23-1, 64-68 cm (#4), Unit P_4. Oscillatory zoning in plagioclase microphenocryst.*

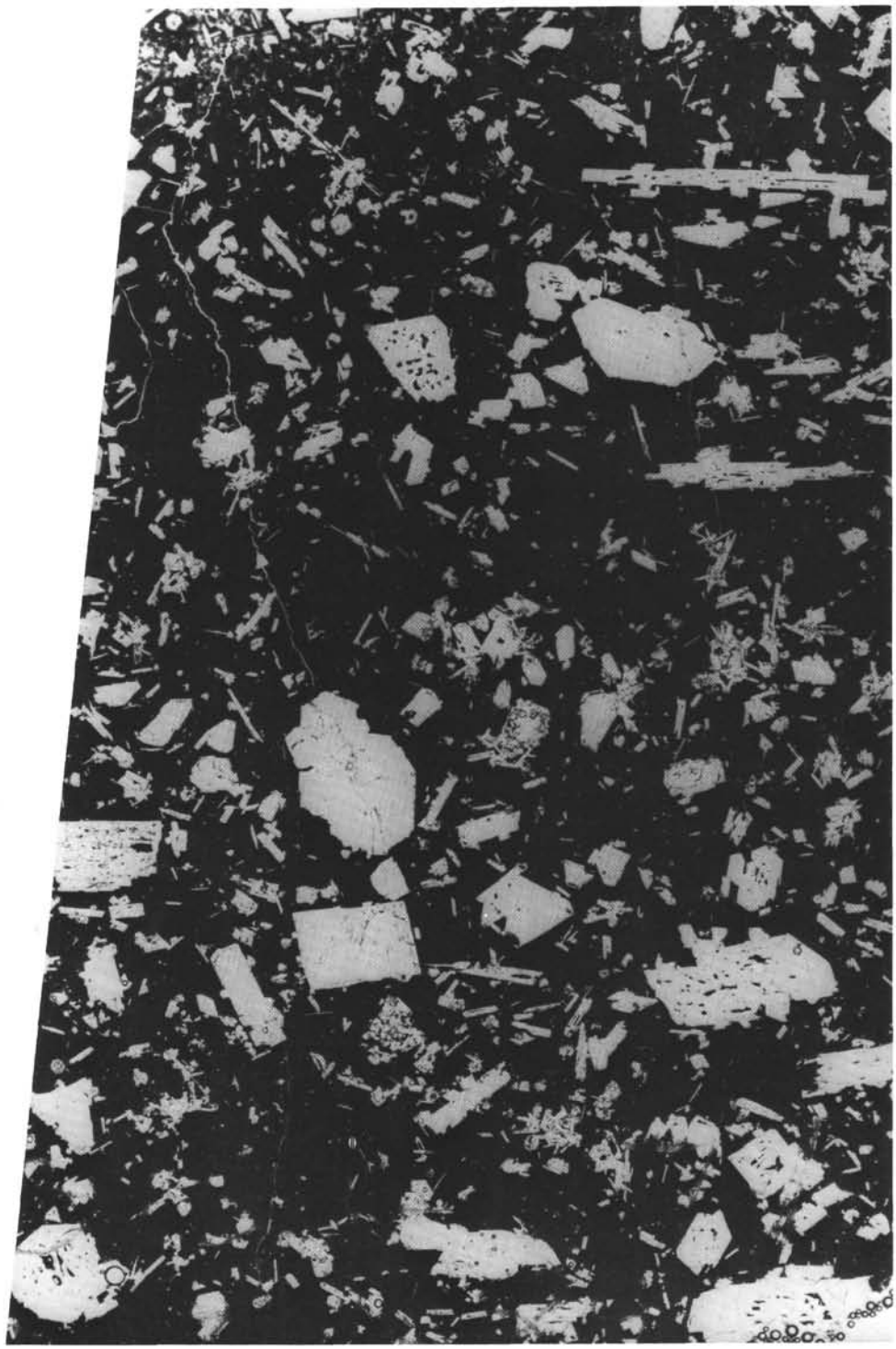

Figure 9. *Sample 395A-17-1, 84-89 cm, Unit P_3. Full thin-section view in transmitted light. Section width about 2.4 cm. Note sub-parallel alignment of many plagioclase crystals (tabular, elongate, many with glass inclusions), and in the center the large irregular glomerocryst without inclusions. Clumps of smaller crystals are second-generation plagioclase and clinopyroxene.*

P_2, P_4, and P_5), no clinopyroxene is definitely intergrown with a first-generation plagioclase, but olivine is (in the dolerite). But olivine and clinopyroxene can be intergrown with second-generation plagioclase. Clinopyroxene, but not olivine, is zoned and shows dendritic margins, reflecting clinopyroxene growth at the fairly extreme undercoolings represented by the typical fine-grained to spherulitic groundmass. Olivine is not present in the groundmass of the finer grained rocks.

Based on mineral relationships and the experiments of Dungan et al. (this volume), there were at least three stages of phenocryst growth in Units P_2, P_4, and P_5. The

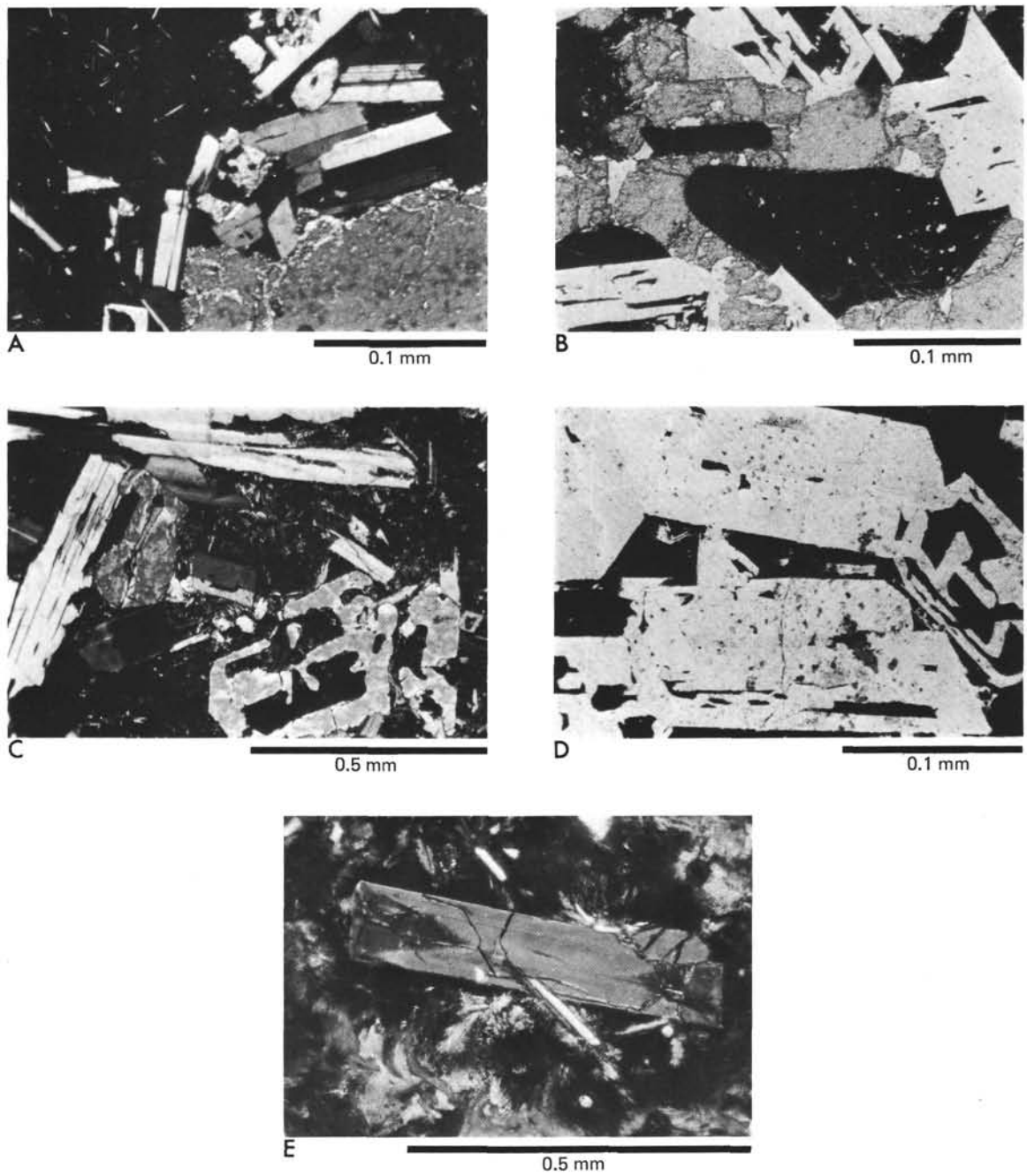

Figure 10. (A) *Sample 395-18-2, 38 cm (#7), Unit P_1. Crossed nicols. Collection of second-generation plagioclase crystals along one side of an olivine megacryst which has a broken, irregular edge.* (B) *Sample 395-18-2, 38 cm (#7), Unit P_1. Crossed nicols. Large embayed olivine crystal partially enclosing plagioclases with skeletal interiors.* (C) *Sample 395-18-2, 38 cm (#7), Unit P_1. Crossed nicols. Skeletal olivine crystal.* (D) *Sample 395-18-2, 38 cm (#7), Unit P_1. Plane polarized light. Associated skeletal olivine and plagioclase crystals.* (E) *Sample 395A-15-1, 55-58 cm, Unit P_2. Crossed nicols. Sector-zoned olivine partially enclosing second-generation plagioclase crystal.*

first occurred in a more "primitive" melt, and resulted in calcic plagioclase and forsteritic olivine with abundant glass inclusions. Even at this stage, some crystal growth was skeletal, resulting in the glass inclusions. At this point, many of the plagioclases underwent partial resorption (Figures 6E and 12). In the model of Dungan et al. (this volume), these melts and their included phenocrysts were then mixed with more fractionated liquids. This apparently produced strong zoning on the feldspars and fractured, fragmented rims on olivine phenocrysts. At this stage, euhedral sodic plagioclase, granular clinopyroxene, and skeletal olivine grew. The small crystal size and the skeletal olivines suggest that this stage involved fairly substantial undercool-

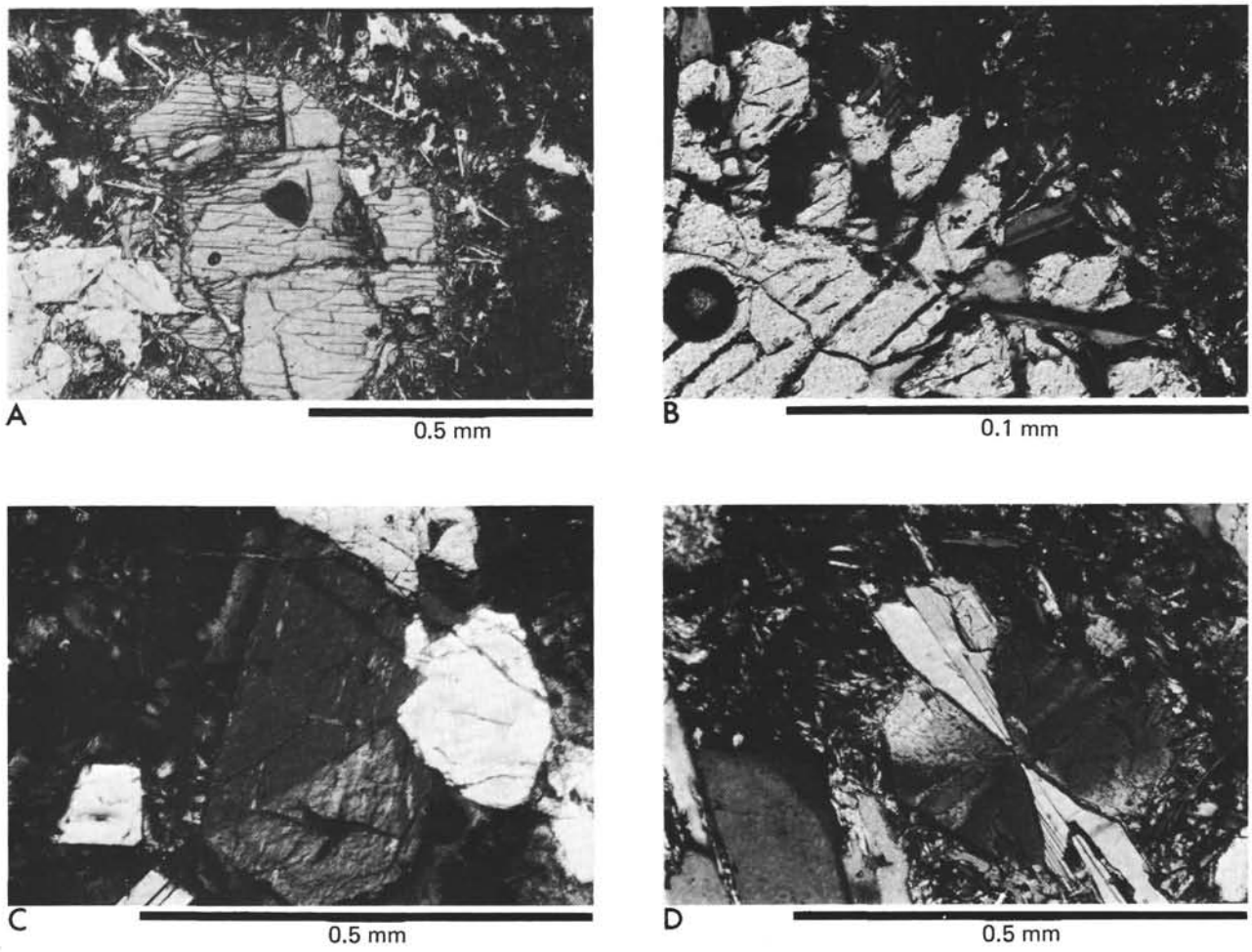

Figure 11. (A) *Sample 395A-23-1, 45-46 cm (#1), Unit P_4. Crossed nicols. Clinopyroxene microphenocryst with dendritic rim intergrown with tiny plagioclases.* (B) *Sample 395A-23-1, 120-121 cm (#12), Unit P_4. Crossed nicols. Detail of dendritic overgrowth on clinopyroxene microphenocryst, showing intergrown plagioclases. Note "staircase." morphology of overgrowth, resembling that of overgrowths on plagioclases in Figures 6C and 6D.* (C) *Sample 395A-16-1, 90-92 cm (#4), Unit P_3. Crossed nicols. Sector-zoned clinopyroxene with an additional zoned rim on one sector. Growth of plagioclase at right may have influenced formation of sector zones.* (D) *Sample 395A-23-1, 64-48 cm (#4), Unit P_4. Crossed nicols. Bow-tie intergrowth of plagioclase and clinopyroxene, apparently producing strong radial zoning in the clinopyroxene*

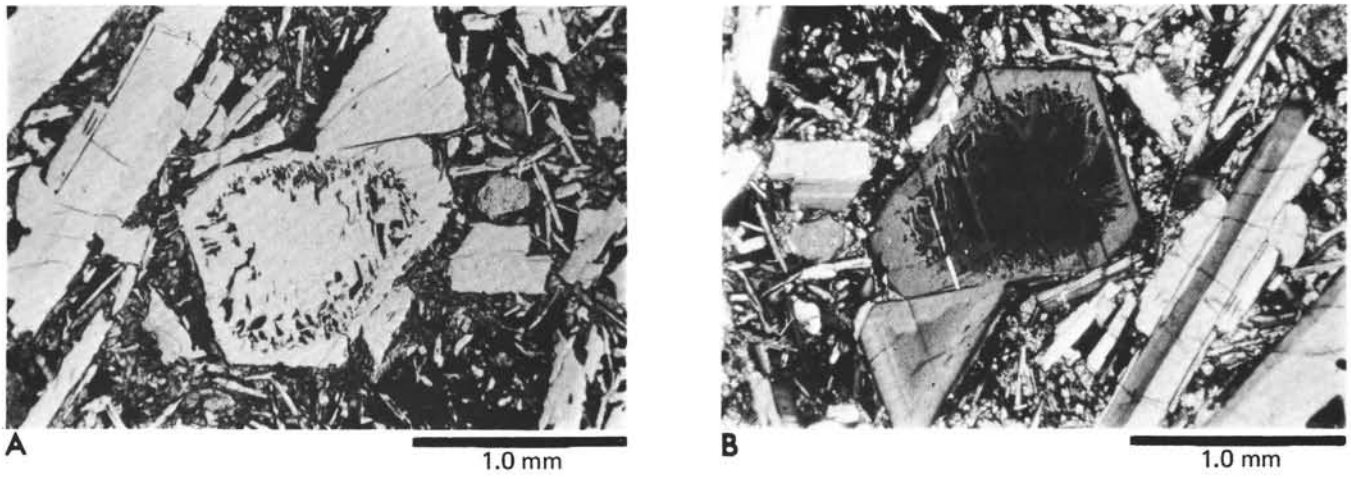

Figure 12. *Sample 395-18-1, 37 cm (#1), Unit P_1. Crossed nicols. Strongly zoned plagioclase phenocryst in fairly well crystallized groundmass. Pitting at edge of inner zone, and its generally rounded outline, suggest that it was partially resorbed before growth of the outer zone.* (A) *Plane polarized light.* (B) *Crossed nicols.*

ings and occurred in a fairly shallow magma reservoir (more on this later). A fair amount of heterogeneous nucleation occurred, producing the glomerocrysts. The final stage was extrusion of the basalts as thin flows and pillows.

Because it is possible that these basalts represent hybrids of two different magma types, one "primitive" and the other "evolved," both containing phenocrysts, the order of crystal growth that can be deduced from the phenocryst varies from rock to rock. At one atmosphere, Dungan et al. (this volume) produced olivine as the second mineral to crystallize (after plagioclase) in an equilibrium crystallization experiment on a Unit P_4 whole-rock composition. Clinopyroxene and titanomagnetite crystallized next after the olivine. In some basalts, indeed, olivine phenocrysts partially enclose euhedral plagioclase, and thus formed after plagioclase. In some glomerocrysts, however, olivine appears to have formed before plagioclase. In other rocks, plagioclase and clinopyroxene are euhedral or granular, and olivine is skeletal, suggesting that it was the third mineral to form. As we shall shortly discuss, plagioclase spherulites are ubiquitous in glassy zones, and are joined in slightly coarser grained basalt by clinopyroxene.

This suggests that the two "end members" which mixed to produce these basalts had fundamentally different equilibrium mineral assemblages. The "primitive" component crystallized first olivine then plagioclase. The "evolved" components crystallized first plagioclase, then clinopyroxene, but no olivine (and in this way are similar to Fe- and Ti-rich ocean ridge basalts). One might then see in the same hybrid rock evidence in glomerocrysts that first-generation olivine had crystallized before first-generation plagioclase, and that skeletal olivine is associated with granular clinopyroxene and euhedral second-generation plagioclase in the surrounding rock. The groundmass might have only plagioclase and clinopyroxene. On the other hand, if the hybrid were predominantly a first-generation composition, there would be no clinopyroxene phenocrysts, and no skeletal olivine. Zoning on first-generation plagioclases would be minor, with less difference in compositions.

These crystal relationships, as complex as they are, apply mainly to the more evolved phyric basalt compositions, Units P_2, P_4, and P_5 (Chapter 7, this volume). The least fractionated phyric basalt units (P_1 and P_3) contain abundant clinopyroxene phenocrysts in addition to olivine and plagioclase. In these basalts, some clinopyroxene appears to be a first-generation mineral. The one-atmosphere experiments of Dungan et al. (this volume) do not apply to these basalts. Though they are interbedded with the more evolved phyric basalts, the contrasting phenocryst assemblages between the two phyric basalt types imply a complex evolution if the two types are co-magmatic. The "primitive" end members inferred to have mixed with more fractionated compositions in Units P_2, P_4, and P_5 carried primarily plagioclase and olivine phenocrysts and glomerocrysts. Yet Units P_1 and P_3 represent still other "primitive" compositions, with three phenocryst phases, and had their own history of hybridization.

A typical sequence of crystallization of minerals in phyric basalts at high undercooling is depicted in a series of photomicrographs showing the development of groundmass textures from the edges to the interior of typical cooling units (Figure 13). Within about 1 cm of glassy rims there are brown spherulites about 0.1 mm in diameter (Figure 13A). These are set in a clear, pale brown glass. Some have tiny central crystallites of plagioclase. They differ from plagioclase spherulites of the A_3 and A_4 basalts in being more perfrectly circular in plan, larger, and lighter brown, and in having a distinct rim about 0.02 mm in diameter. This same brown spherulitic material nucleates both on tiny crystallites and on plagioclase phenocrysts of any size (Figures 13B and 13C). No olivine spherulites occur in any phyric basalt.

About 2 cm from cooling unit boundaries, plagioclase growth is sheaf- (or bow-tie) spherulitic (Figure 13D). Tiny titanomagnetites are concentrated at the ends of the fan-like sheafs. Clinopyroxene is probably present, but is masked by the brown of the spherulitic bundles.

Still farther into cooling units (probably >10 cm), groundmass crystal morphologies are skeletal for plagioclase, spherulitic and dendritic for clinopyroxene, and skeletal for titanomagnetite (Eisenach, this volume), as shown on Figures 13E and 13F. In the larger cooling units (thick flows and the dolerite intrusions), plagioclase becomes euhedral and tabular, but clinopyroxene is still largely dendritic (Figure 13G). At distances several meters from cooling-unit boundaries, textures are sub-ophitic, and plagioclase encloses granular clinopyroxene and skeletal titanomagnetite (Figure 13H). In some, but not all, coarse-grained rocks, granular olivine can be seen in the groundmass.

Olivine, then, does not appear to have grown in the groundmass at any condition of undercooling represented by extrusive pillow lavas or thin flows, but does occur in thicker flows and in the fairly shallow doleritic intrusives (originally about 300 m below the sea floor, assuming time equivalence to chemically similar phyric Unit P_4). This contrast with the aphyric basalt units can partly be explained by the higher CaO of phyric glasses compared with aphyric glasses (Melson, this volume). Many phyric basalt glasses also have lower Na_20 and TiO_2. Thus, plagioclase, rather than olivine or clinopyroxene, is the liquidus mineral in these basalts, and grew as euhedral crystals and coarse dendritic rims on phenocrysts much closer to cooling-unit boundaries than plagioclase of similar morphologies in the aphyric basalts. The high CaO also favored uptake of MgO into clinopyroxene, thus contributing to the suppression of olivine crystallization.

PHENOCRYSTS AND GLOMEROCRYSTS IN THE DOLERITES

Thin sections from the dolerite sections deep in Hole 395A (lithologic Units 20 and 22) demonstrate clearly that there are two intrusive bodies, both with fine-

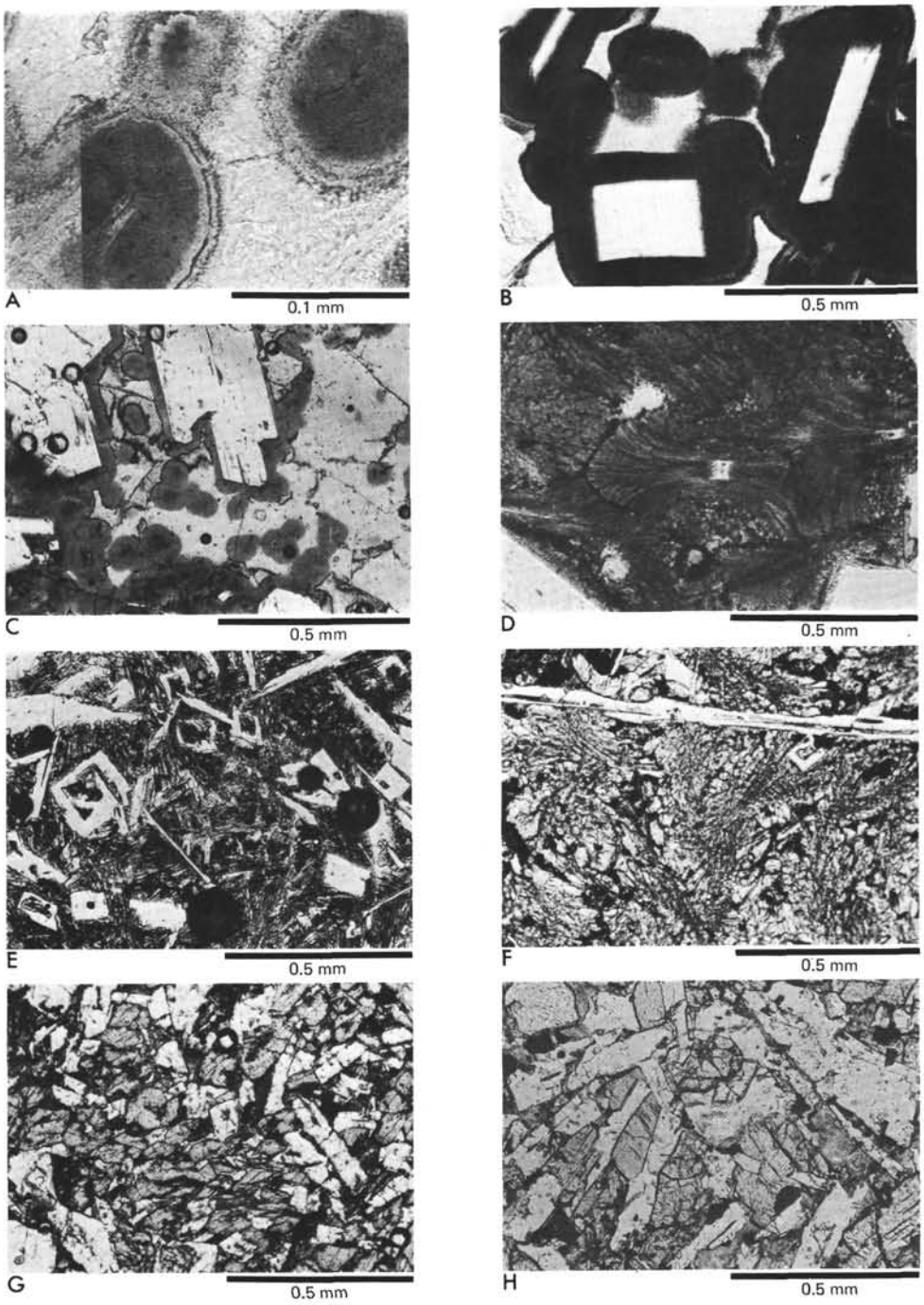

Figure 13. *Sequence of photomicrographs showing range of groundmass textures in a variety of phyric basalts. Glassiest basalts contain only pale brown plagioclase spherulites* (A *through* C). *The same spherulitic brown fibrous material rims phenocrysts* (B, C) *A few centimeters farther into pillows, plagioclase fan-spherulites are well developed* (D). *Probably many of the fibers here are clinopyroxenes. As rocks become coarser* (E *through* H), *plagioclase changes from skeletal* (E, F) *to tabular* (G, H), *and clinopyroxene from spherulitic* (E) *to dendritic* (F, G) *to granular, sub-ophitically intergorwn with plagioclase and surrounding an olivine crystal* (H). (A) *Sample 395A-17-1, 131-132 (#15D), Unit* P_3; (B) *Sample 395A-16-1, 90-92 (#4), Unit* P_3; (C) *Sample 395A-17-1, 131-133 (#15D), Unit* P_3; (D) *Sample 395A-15-1, 55-58, Unit* P_2; (E) *Sample 395A-31-1, 83-87 (#6), Unit* P_5; (F) *Sample 395A-20-1, 142-144 (#1); Unit* P_3; (G) *Sample 395A-32-1, 35-36 (#3), Unit* P_5; (H) *Sample 395A-14-1, 90-100 (#12), Unit* P_2. *All pictures were taken in plane polarized light.*

grained (but not glassy) margins and coarse-grained subophitic interiors. Their intrusive nature is inferred from (1) chemical equivalence to phyric Unit P_4 higher in the section (Bougault et al., this volume; Rhodes et al., this volume); (2) remagnetization of basalts below the lower dolerite (Johnson, "Paleomagnetism of igneous rocks," this volume); and (3) oxygen-isotope evidence for formation of secondary minerals at temperatures near 15°C above the dolerites, and between 30° and 40°C below them (Lawrence et al., this volume).

Several features of the dolerites are worth mentioning from a petrographic point of view. First, megacrysts of first-generation zoned plagioclase containing glass inclusions are both larger and more abundant in the interior than at the edges of the dolerites (Figures 14 and 15). Second, rare phenocrysts of olivine and clinopyrox-

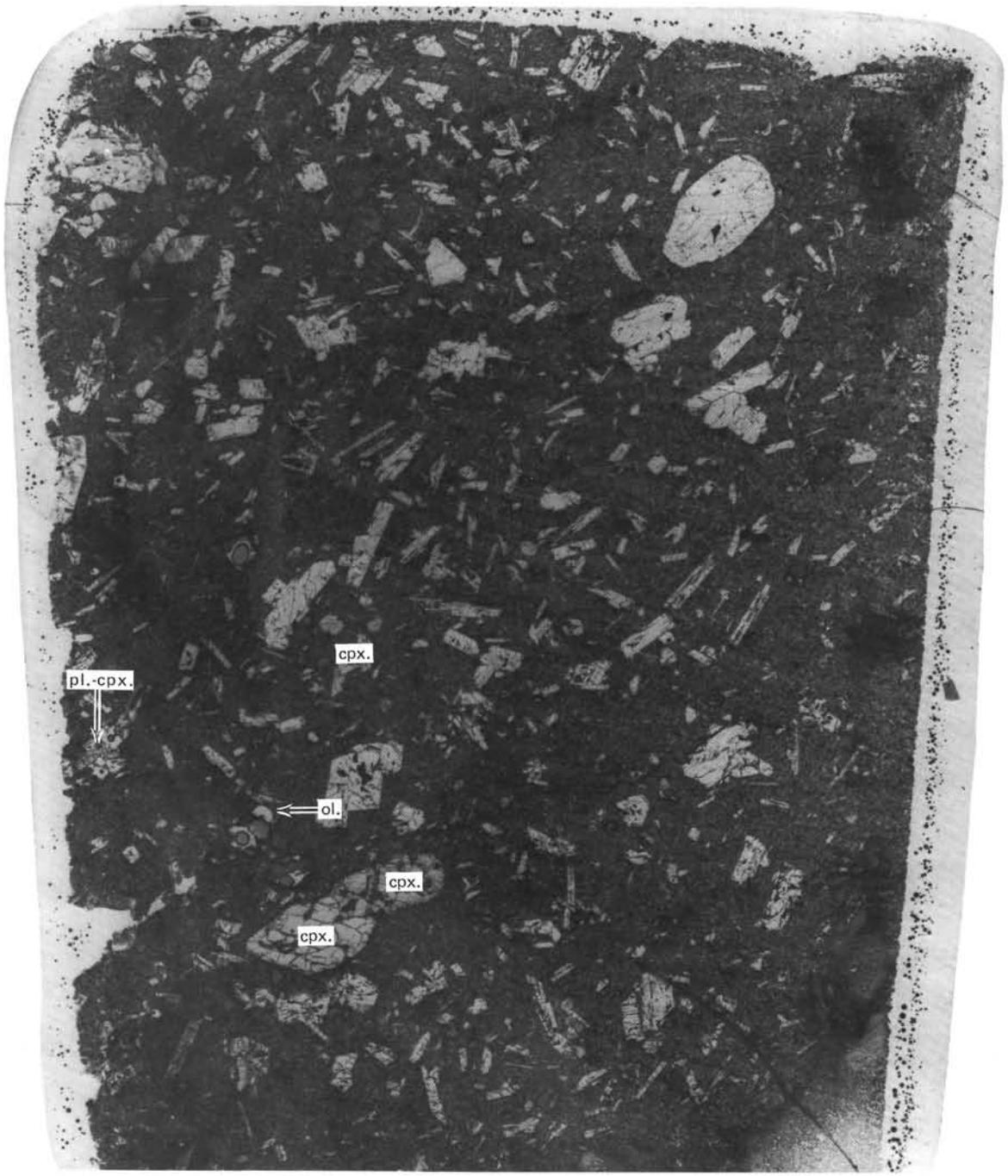

Figure 14. *Full thin-section photomicrograph of upper chilled margin of lower dolerite. Sample 395A-62-1, 80-87 cm (#7B). Transmitted light. Longest dimension is equivalent to 3.2 cm. Rounded crystal in corner is plagioclase. The larger mafic minerals (olivine = ol, clinopyroxene = cpx) are shown, but many smaller ones, especially clinopyroxene, occur. Skeletal crystals are all plagioclases.*

Figure 15. *Full thin-section view of the interior of the lower dolerite, Sample 395A-63-1, 40-43 cm (#3D). Transmitted light. Longest dimension is equivalent to 3.0 cm. Rare isolated olivines (ol) are indicated. Skeletal crystals are plagioclase megacrysts.*

ene occur near the fine-grained margins, but not in the interiors of the dolerites. Third, large glomerophyric intergrowths of plagioclase and olivine are concentrated toward the bottom of the intrusives, along with large individual crystals of plagioclase and olivine (Figure 16). Both the plagioclases and the olivines contain glass inclusions, and are therefore "first-generation" minerals.

These relations indicate that gravitational settling of the glomerophyric clumps was occurring in the dolerites, so they are not vertical, and that the large plagioclase megacrysts were first concentrated toward the centers of the intrusives, probably by flow differentiation. Crystal settling in the dolerites was also demonstrated by Propach et al. (this volume).

The extrusive phyric basalt Units P_1 through P_5 interestingly enough exhibit some of these same contrasts. One nearly glassy basalt of Unit P_4 is charged with large glomerocrysts (Figure 17), yet in another basalt from Unit P_4 they are absent (Figure 18). It is therefore evident that some of the size sorting of phenocrysts and glomerocrysts is manifested in the extrusive stage of these basalts, and can be ascribed to a combination of gravitational crystal settling and, possibly, flow differentiation before extrusion.

One other aspect of the plagioclase phenocrysts in the dolerites is worth noting. The plagioclases associated with olivine in the glomerophyric clumps either are only slightly skeletal or are not skeletal at all. By contrast,

Figure 16. *Full thin-section view of lower chilled margin of lower dolerite, Sample 395A-64-2, 116-122 cm. Transmitted light. Abundant and fairly large individual olivines, and olivines with plagioclase in glomerocrysts, are indicated (ol). Note relative lack of skeletal plagioclases compared with Figure 15, and large dark spherulitic inclusions in the largest olivine and glomerocryst.*

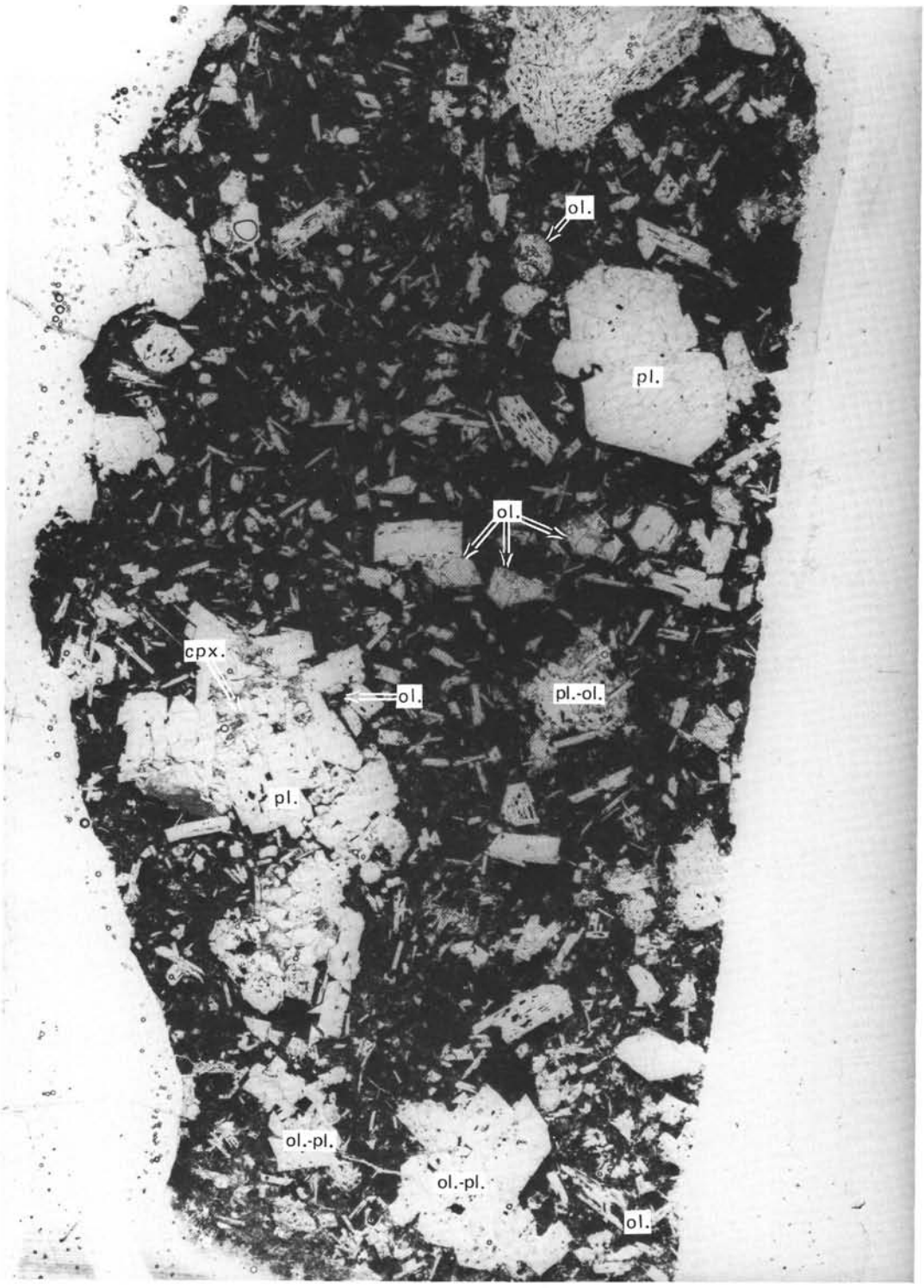

Figure 17. *Full thin-section view of portion of pillow in Unit P_4 Sample 395A-24-2, 124-130 cm (#2). Transmitted light. Longest dimension equivalent to 3.6 cm. Large olivines (ol) and non-skeletal plagioclase (pl) in glomerocrysts are shown.*

the isolated first-generation plagioclases are riddled with glass inclusions, indicating skeletal growth. This implies that the more calcic plagioclases, not just the sodic plagioclases, grew at a range of undercoolings. We might therefore speculate that at least two fairly large slowly cooled magma reservoirs were involved in the evolution of the phyric basalts, one allowing glomerocrysts of the more calcic plagioclase and the forsteritic olivine to form, the other allowing glomerocrysts of the more sodic plagioclases to form. Periodically, magmas

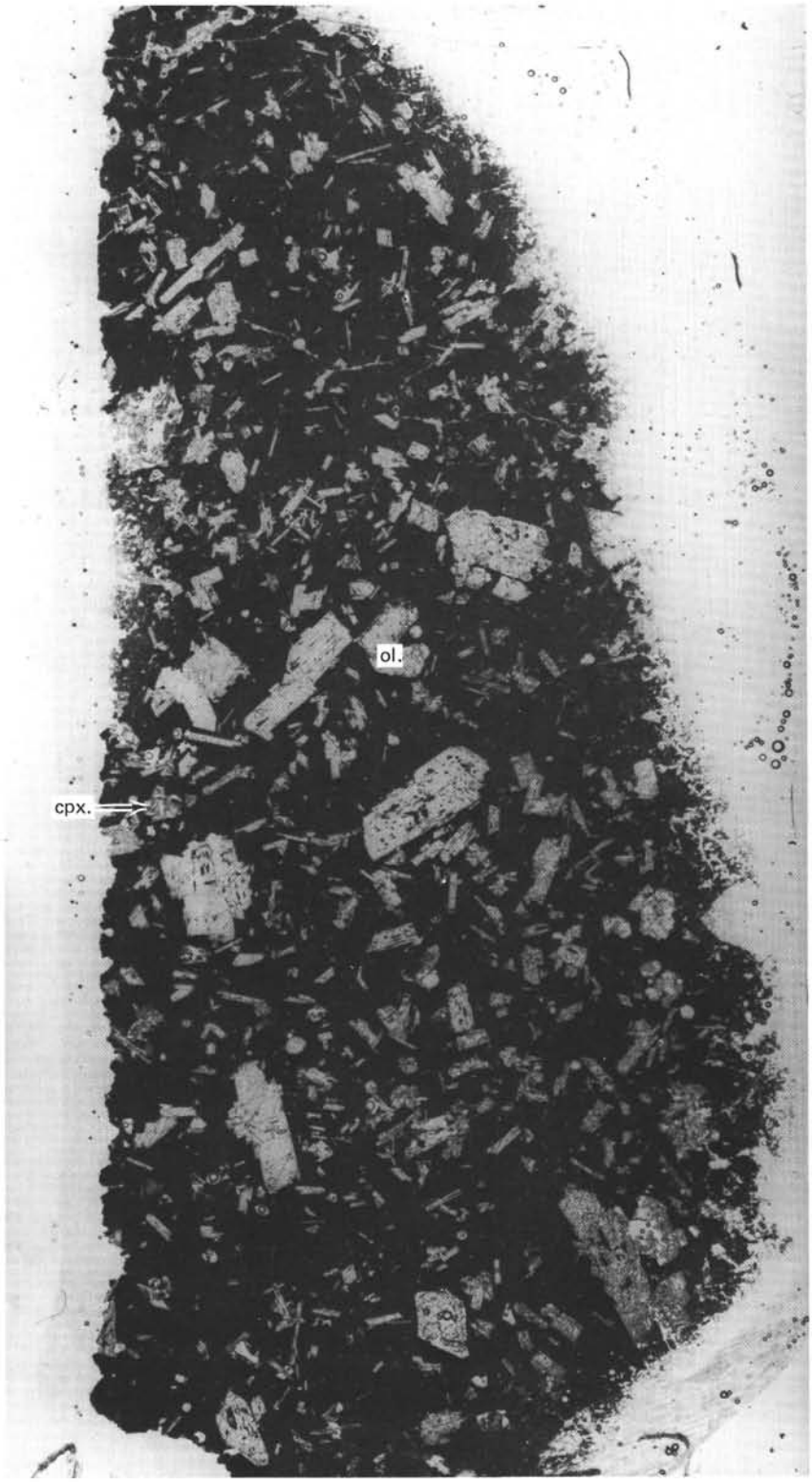

Figure 18. *Full thin-section view of portion of pillow in Unit P_4, Sample 395A-27-2, 69-78 cm (#4). Transmitted light. Longest dimension equivalent to 2.9 cm. Largest olivine (ol) and clinopyroxene (cpx) crystals are shown. Other large crystals are plagioclase.*

from the first were injected into the second, and it was during the transit between the two that the skeletal calcic plagioclases formed. Once inside the second reservoir, more sodic but non-skeletal zones formed around the calcic plagioclase cores. This effect was most pronounced when the proportion of introduced magma was small, or the contrast in compositions between the two magma types was extreme, because in some basalts little zoning can be seen. The period of transfer between the two reservoirs was a period of heightened undercooling which promoted skeletal growth. The transfer could have been either lateral or vertical, but the skeletal calcic plagioclases might be evidence for lateral transfer. Jaeger (1968) calculated that the country rock midway between two parallel molten intrusive sheets, one above the other, could become considerably hotter than the rock at the same distance either below or above the sheets and remain so for a longer time. How hot it gets, and how long it remains hot depends, of course, on the thickness of the sheets and the distance between them. But in a setting of rapid production of magmas and steep thermal gradients within the crust, a vertical conduit between two such bodies would not be a likely place to maintain high cooling rates. Instead, we may here have an analog of the Kilauea rift system, in which relatively unfractionated magmas branch laterally from a main conduit system and encounter pockets of fractionated magmas far out along the rift (Fiske and Jackson, 1971; Wright, 1971). Supporting this is the idea that the magmas within the inferred second reservoir were more fractionated than those that invaded it; that some crystals within the invading magma were skeletal, implying heightened undercooling during the transfer process; and that phenocrysts and glomerocrysts native to the second reservoir were considerably smaller than most of the introduced phenocrysts. In fact, the typical second-generation plagioclase phenocryst size (either as single crystals or within glomerocrysts) is about the same (0.1 to 0.5 mm) as plagioclases which crystallized between 12.8 and 16.5 meters depth in Makaopuhi lava lake, Kilauea volcano, Hawaii (Kirkpatrick, 1976). Here, too, nucleation was predominantly heterogeneous on pre-existing crystals.

From the cooling-rate experiments of Dungan et al. (this volume), one can get some idea of the cooling rates at which various crystal morphologies were produced in the phyric basalts. At 30°/hr, skeletal plagioclase needles grew in a spherulitic matrix. And at 2°/hr, plagioclase laths and subhedral olivine were set in an olivine, plagioclase, and spherulitic-clinopyroxene matrix. Even at the slowest of these cooling rates, the magmas would be entirely consolidated within a few days. The experiments therefore cannot possibly bear on the consolidation of larger magma bodies, given that Makaopuhi lava lake (about 83 m deep) was producing crystals similar in size to the phyric basalt second-generation plagioclase, at a depth of 16.5 meters, fully 12 months after formation of the lake. The cooling-rate experiments, however, are probably pertinent to the consolidation of pillows and thin flows, which exhibit this range of crystal morphologies. The interiors of the thicker flows and the dolerites, though, apparently grew at considerably lower cooling rates than 2°/hr, since textures are sub-ophitic, with plagioclase surrounding well-formed, not dendritic, clinopyroxene.

The critical question which the cooling-rate experiments do not answer is, what cooling rates are implied by the skeletal first-generation plagioclase crystals? If cooling rates were between 2°/hr and 30°/hr, then the transfer conduits must indeed have been shallow, probably within the upper few hundred meters of crust cooled by circulating sea water. The dolerite intrusions, which were probably overlain by about 300 meters of basalt at the time of their injection, do not have comparable skeletal textures in second-generation plagioclases even 1 meter from their margins. Since they have the composition of phyric basalt type-P_4 extrusives, and contain both first- and second-generation phenocrysts, they, too, are evidently hybrids. The dolerites thus do not represent conduits between the two inferred magma reservoirs; they are dikes or sills emanating from the second reservoir.

Another problem not completely resolved at this time is that the Sr contents of the phyric basalts are not consistent with their being co-magmatic with each other, nor with any basalt resembling the aphyric basalts. Ni and Cr appear to be diluted 15 to 25 per cent, relative to aphyric basalts, by plagioclase phenocrysts (Chapter 7, this volume; Bougault et al., this volume), but the extent of this dilution is not consistent. It can be more in a rock whose Ni, Cr, and Zr indicate an unfractionated composition than in a fractionated rock, and vice versa.

In the mode, plagioclase phenocrysts range between 15 per cent and 25 per cent, and at first sight, this might explain the dilution effect. But it is obvious that plagioclase is the liquidus phase in these rocks and that the second-generation plagioclases in particular are probably not accumulative. Phenocrysts in the coarser grained rocks are all first-generation minerals, and the second-generation plagioclase phenocrysts grew at all stages of undercooling through the extrusion of the basalts except the consolidation of small pillows. They thus belong "in the basalts."

In any phyric basalt, first-generation plagioclase phenocrysts probably amount to no more than half the total plagioclase phenocryst content, and usually less. Although they have been introduced by magma-mixing processes, and their concentration in any given phyric basalt may have been increased by crystal settling (usually in glomerocrysts also containing olivine) and flow-differentiation, it is doubtful that the full magnitude of the "Sr anomaly" can be explained entirely by these processes. Two other effects might be responsible.

Sr in the phyric basalts might be concentrated in secondary minerals, such as calcite in cracks and along mineral boundaries (Bougault et al., this volume). It is not clear why this would be so much more pronounced in phyric basalts than aphyric basalts, especially when in their overall aspect they are just as fresh.

Sr might be fundamentally more abundant in these basalts than in the aphyric basalts. Sr, of course, does not behave as an incompatible element with respect to

plagioclase, either during melting or during crystal fractionation. The phyric basalts have plagioclase alone on the liquidus, whereas the aphyric basalts have olivine, or olivine closely followed by plagioclase. This suggests that more of the components of plagioclase were selectively incorporated into the parents of these phyric basalts during melting than into the aphyric basalt "parents." The result might have been higher concentrations of Sr in the original melts, diluting high-partition coefficient elements such as Ni and Cr. Zr and TiO_2 contents are lower with respect to Ni and Cr in the phyric basalts than in the aphyric basalts, suggesting that the phyric basalts were produced by greater partial melting in the mantle (Chapter 7, this volume; Bougault et al., this volume).

A final question to consider is whether the various magma types, phyric and aphyric, could represent repeated eruptions from the same magma reservoir. On balance, I believe that at least two magma reservoirs must have been involved. The three aphyric types differ so subtly in composition (Chapter 7, this volume) that they could well have come from the same reservoir, replenished episodically from deeper sources to produce the small compositional differences. Sufficient time elapsed between eruptions (Johnson, Paleomagnetism of Igneous Rocks, this volume) to erase all evidence of hybridization or internal fractionation. There are essentially no phenocrysts, and no internal chemical trends either, to indicate fractionation or mixing between old and new chemical types. In every respect, the aphyric basalts are compositionally discrete.

The phyric basalts, on the other hand, have every possible mineralogical evidence for magma mixing, and neither group of "primitive" or "evolved" end-members of these hybrid rocks resembles the aphyric basalts. Substantial differences still exist in contents of CaO, Na_2O, TiO_2, and Ni/Zr (Bougalt, et al., this volume. Differences also exist in contents of CaO, Na_2O, and TiO_2 in the glasses (Melson, this volume). This probably reflects at least a basic difference in the extent of melting in the mantle (higher in the phyric basalts; Bougault et al., this volume). In addition, a range in sizes of magma reservoirs in an interrelated network appears necessary to explain the variety of phenocryst morphologies and sizes. Phenocrysts have been *concentrated* in the phyric basalts by mechanical processes (accumulation, flow differentiation, etc.). In the aphyric basalts, they either were never present, or they have been *eliminated.* This alone indicates fundamentally different fluid dynamic processes, which would be critically affected by the size and shape of reservoirs and conduits, and by the rate of flow of magma. Apart from all of these is the stratigraphic fact of aphyric basalt units both below *and* above the phyric basalts. The basic plumbing and rate of supply for aphyric basalt types thus was not disrupted by the interval of phyric basalt eruptions. Most probably, then, two independent source and conduit systems were involved, closely spaced in the median rift of the Mid-Atlantic Ridge near Site 395 about 7 million years ago.

ACKNOWLEDGMENTS

I would like to thank Bill Melson for thoughtful and provoking discussion about the significance of crystal morphologies, on board the *Challenger* during Leg 45, and Jim Kirkpatrick for properly introducing me to the subject and for reviewing the manuscript. I am indebted to the fine staff of marine technicians on Leg 45 who all participated in making the thin sections used for this study.

REFERENCES

Bryan, W.B., 1972. Morphology of quench crystals in submarine basalts, *J. Geophys. Res.*, v. 77, p. 5812-5819.

Donaldson, C.H., 1976. An experimental investigation of olivine morphology, *Contrib. Mineral. Petrol.*, v. 57, p. 187-213.

Fiske, R.F. and Jackson, E.D., 1972. Orientation and growth of Hawaiian volcanic rifts: the effects of regional structure and gravitational stresses, *Phil. Trans. Roy. Soc. London Proc.*, v. 329, p. 399-326.

Jaeger, J.C., 1968. Cooling and solidification of igneous rocks, *In* Hess, H.H. and Poldervaart, A. (Eds.), *Basalts,* v. 2: New York (Wiley Interscience), p. 503-536.

Johnannsen, A., 1939. *A descriptive petrography of the igneous rocks:* Chicago (Univ. Chicago Press), v. 1, p. 1-318.

Kirkpatrick, R.J., 1977. Nucleation and growth of plagioclase, Makaopuhi and Alea lava lakes, Kilauea Volcano, Hawaii, *Geol. Soc. Am. Bull.*, v. 88, p. 78-84.

Lofgren, G., 1971. Spherulitic textures in glassy and crystalline rocks, *J. Geophys. Res.*, v. 76, p. 5635-5648.

_____, 1974. An experimental study of plagioclase crystal morphology: isothermal crystallization, *Am. J. Sci.*, v. 274, p. 243-273.

Walker, D., Kirkpatrick, R.J., Longhi, J., and Hays, J.F., 1976. Crystallization history of lunar picritic basalt sample 12002: Phase-equilibria and cooling-rate studies, *Geol. Soc. Am. Bull.*, v. 87, p. 646-656.

Wright, T.L. and Fiske, R.S. 1971. Origin of differentiation and hybrid lavas of Kilauea Volcano, Hawaii, *J. Petrol.*, v. 12, p. 1-65.